INSTITUTE OF PLASMA PHYSICS

NAGOYA UNIVERSITY

Stochasticity of Phase Trajectory of a Charged Particle in a Plasma Wave

Akihiko MURAKAMI, Yasuyuki NOMURA

and Hiromu MOMOTA

(Received - May 23, 1980)

IPPJ-464 June 1980

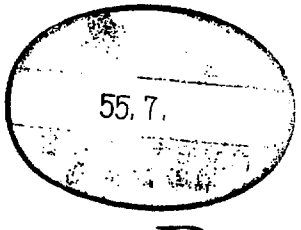

RESEARCH REPORT

NAGOYA, JAPAN

Stochasticity of Phase Trajectory of a Charged Particle in a Plasma Wave

Akihiko MURAKAMI, Yasuyuki NOMURA
and Hiromu MOMOTA

(Received - May 23, 1980)
IPPJ-464 June 1980

Further communication about this report is to be sent to the Research Information Center, Institute of Plasma Physics, Nagoya University, Nagoya 464, Japan

Abstract

Stochastic behavior of charged particles in finite amplitude plasma waves is examined by means of particle simulations under the condition that Chirikov's criterion is broken down. The process of growing the stochastic region is clarified and accordingly the width of the stochastic region is discussed. Discussions on the effects of higher order resonances are also presented.

1. Introduction

The problem of analyzing phase trajectories of charged particles in a plasma wave has been studied by many authors.[1~6] Especially the analysis of phase trajectories in a monochromatic and finite amplitude plasma wave with a small perturbation has been interested in.[3~6] In an early theory,[1] phase trajectories of charged particles in a constant and finite amplitude monochromatic plasma wave has been analyzed. Particles have been classified into two classes by a boundary called separatrix: the trapped particles inside the separatrix and the untrapped ones outside the separatrix. In recent papers,[3~6] the influence of a small perturbation, which comes from a small travelling wave or a small oscillation of amplitude, on trajectories of charged particles has been analyzed on the basis of a perturbation theory. It has been shown that the main result of the influence of the perturbation is formation of a stochastic region[7] in the vicinity of the separatrix of the unperturbed wave. The motion of a particle in this region is called stochastic, i.e., the particle wanders about this region. In this stochastic region, the above-mentioned classification loses its meaning and the distribution of particles is flattened[4] as time goes on.

In this perturbation scheme, the onset of stochasticity of phase trajectories has been estimated by using so-called "Chirikov's resonance overlapping criterion".[7~9] This "Chirikov's criterion" is expressed as follows: there exists an evaluation function P called "the stochastic parameter", such

that (1) in order that a given "resonance surface" remains adiabatic (non-stochastic) it is necessary that the condition $P<<1$ holds on that surface, and (2) in the region where "resonance surfaces" are dense the stochastic region is determined by the condition $P \gtrsim 1$.

However, for example, in the case of a finite amplitude oscillating wave, the magnitude of the perturbation may exceed the applicable range of the perturbation scheme. Therefore the applicability of Chirikov's criterion to this case may become a subject of discussion. As concerns the applicability of the condition (1), A.B.Rechester and T.H.Stix[6] have shown its validity in the case of a travelling wave by computer simulations. The validity of the condition (2) may become significant because of the fact that the area of the stochastic region plays important roles in recurrence of the oscillating amplitude.

The purpose of this paper is to study the applicability of the perturbation scheme to the case of the amplitude oscillating wave. The appearance of the stochastic region is also discussed. For this purpose the potential amplitude is assumed as follows:

$$\Phi(t,x) = \Phi(1 + \varepsilon \cos \omega_b t) \cos(\kappa x - \omega t) \quad , \qquad (1.1)$$

$$\varepsilon < 1 \quad . \qquad (1.2)$$

Here the quantities κ and ω are the wave number and frequency of the unperturbed wave, respectively. And the quantity ε is the depth of modulation and the frequency of the modulation is assumed to be a bounce frequency $\omega_b = \sqrt{e\Phi/m}$.

In Sec.2 one-dimensional electrostatic particle code is employed for the purpose of studing phase trajectories of charged particles in a self-consistent field. At the same time, the area of the stochastic region is estimated. In Sec.3 the area of the stochastic region is analyzed according to the perturbation scheme. The results are compared to that obtained in Sec.2 where the magnitude of the perturbations exceeds the applicable range of Chirikov's criterion. In Sec.4 numerical calculations are executed in order to obtain some relation between the area of the stochastic region and the parameter ε with wide range. From these numerical results the dependence of the width of the stochastic region on the value ε is obtained and the appearance of the stochastic region is examined. These results support the validity of Chirikov's resonance overlapping scheme. Section 5 is devoted to the summary of the results and some discussions on evolution of the width of the stochastic region and effects of higher order resonances.[8,9]

2. Phase Trajectories of Charged Particles and the Stochastic Region in a Self-consistent Field

In this section particle trajectories in a finite amplitude plasma wave are investigated by self-consistent computer simulations. One-dimensional electrostatic particle code is employed, and motions of electrons are calculated as follows: Ions are assumed to constitute a fixed uniform neutralizing background.

A periodic boundary condition is adopted for field quantities and particle motions. In order to reduce the fluctuations and collisional effects due to the discreteness of particles, 96000 particles are employed and "Quiet-Start" technique is introduced.

The initial distribution function is assumed to be, $f(x,v,t=0) = f_0(v)+f_1(v)\cos(\kappa x)$, where $f_0(v)$ is the Maxwellian distribution function and $f_1(v)$ is determined from a solution of linearized Vlasov's equation corresponding to the initial electric field. In order to avoid divergence, $f_1(v)$ is assumed to be zero for the resonant particles because the electric field is produced by the main plasma and the resonant particles make a negligible contribution to it.

The parameters are chosen as follows: Time step Δt is 0.2 and system size L(the wave length of the initial electric field) is 32. Here the time and the length are normalized by the inverse of the plasma frequency ω_{pe}^{-1} and the grid spacing Δ, respectively. The thermal velocity of the Maxwellian distribution V_t is approximately 1.6, the phase velocity V_{ph} is $3.5V_t$ and consequently the system length is approximately $20\lambda_D$, where λ_D denotes the Debye length.

The numerical experiments are carried out for various values of initial amplitude Φ_0: for the case (a) of a small amplitude, $e\Phi_0=0.22T_e$ and for the case (b) of a lage amplitude, $e\Phi_0=0.56T_e$, where T_e denotes the electron temperature. Time evolution of the amplitude of the waves are shown in Figs.1 (a) and (b), where the values are normalized by Φ_0 and averaged out by the time interval 2.6.

The amplitude of these examples strongly damps initially because of the Landau damping mechanism, but evolution of the amplitude after initial one period may support the idealized expression (1.1) for the amplitude oscillating wave: the amplitude oscillates around a constant value Φ_∞ which corresponds to the amplitude of the unperturbed wave. Here the ratio Φ_∞/Φ_0 is 0.48 in the case (a) and 0.33 in the case (b). The averaged period of the amplitude oscillations is 73.3 in the case (a) and 56.7 in the case (b). Since the bounce time T_b ($T_b=2\pi/\omega_b$, where $\omega_b= \kappa\sqrt{e\Phi_\infty/m}$) is 62.7 in the case (a) and 48.1 in the case (b), the frequency of the modulation can be regarded as ω_b. The depth of the modulation ε decreases its magnitude gradually due to the mixing of the particle distribution. The averaged value of ε is 0.34 in the case (a) and 0.3 in the case (b).

The examples of particle trajectories are exhibited in Figs.2 (a) and (b) corresponding to the small amplitude wave (Fig.1 (a)) and the large amplitude wave (Fig.1 (b)), respectively. A dotted curve stands for the separatrix of the corresponding asymptotic value of the amplitude Φ_∞. In both figures, type (i) illustrates the adiabatic motions, and type (ii) the stochastic motion in the self-consistent field.

The area of the stochastic region can be estimated by tracing the motion of type (ii). Figures 3 (a) and (b) demonstrate these stochastic regions formed by the wave after initial one period. The particles which are located initially in the hatched region behave stochastically, and in the other region adiabatically. The dashed curves stand for the separatrix. The area

of the stochastic regions is estimated as follows:

(a) $0.34I_0$ (inside the separatrix)
and $0.19I_0$ (outside the separatrix),

(b) $0.35I_0$ (inside the separatrix)
and $0.27I_0$ (outside the separatrix),

where I_0 denotes the area bounded by the separatrix.

Next, evolutions of particle distributions near the phase velocity of the unperturbed wave are visualized in the phase plane. The initial Maxwellian distribution is exhibited in Fig.4. After the waves are turned on, a group of particles is bounced in the potential and finally these particles are distributed uniformly near the separatrix. These characteristics are demonstrated in Figs.5 (a) and (b), respectively, for the case of a small amplitude and a large amplitude. In these figures the distribution at time T_1, one period of amplitude oscillation after the waves are turned on, and T_2, a half period after T_1, are exhibited. The distributions of the final states are also exhibited in these figures.

3. Analysis of Phase Trajectories and Formation of the Stochastic Region based on the Perturbation Theory

In this section, formation of the stochastic region by the amplitude oscillating wave given by (1.1) is discussed analytically according to the perturbation scheme.

The equations of motion for a charged particle is written as

$$\frac{dX}{dT} = V \quad , \tag{3.1}$$

$$\frac{dV}{dT} = -(1 + \varepsilon \cos T) \sin X \quad . \tag{3.2}$$

Here the reference frame moving with the phase velocity of the unperturbed wave is chosen, and the quantities T and X stand for the time and the position normalized by the bounce period ω_b^{-1} and the wave length κ^{-1}, respectively.

The basic equation is described in terms of the following Hamiltonian:

$$H(V,X,T) = H_0(V,X) + H_1(V,X,T) \quad , \tag{3.3}$$

$$H_0(V,X) \equiv \frac{1}{2} V^2 - \cos X = W \quad , \tag{3.4}$$

$$H_1(V,X,T) \equiv - \varepsilon \cos T \cos X \quad , \tag{3.5}$$

where $H_0(V,X)$ is the time independent unperturbed Hamiltonian and W is the corresponding energy eigenvalue. The function $H_1(V,X,T)$ is a time dependent Hamiltonian and assumed to be a small perturbation. According to the value of W, the phase plane is divided into two regions by the separatrix(W=1). The quantity W satisfies an inequality $-1<W<1$ inside the separtrix, and $W>1$ outside the separatrix.

Theoretical treatment of (3.4) is easy in action-angle variables, I and Θ. The action variable I is defined as

$$I \equiv \frac{1}{2\pi} \oint V \, dX \quad . \qquad (3.6)$$

The canonical conjugate angle variable Θ is given by

$$\Theta \equiv \frac{\partial S(X,I)}{\partial I} \quad , \qquad (3.7)$$

by using the generating function

$$S(X,I) \equiv \int^{X} V(X',I) \, dX' \quad . \qquad (3.8)$$

Then the unperturbed Hamiltonian H_0 is described by the variable I alone, and equations of the unperturbed motion are rewritten as

$$\frac{dI}{dT} = - \frac{\partial H_0}{\partial \Theta} = 0 \quad , \qquad (3.9)$$

$$\frac{d\Theta}{dT} = \frac{\partial H_0}{\partial I} \equiv \Omega(I) \quad . \qquad (3.10)$$

In each side of the separatrix, I, Θ, and $\Omega(I)$ are represented in terms of elliptic integrals as follows:

inside the separatrix,

$$I = \frac{8}{\pi} \{ E(b_i) - (1-b_i^{\,2})K(b_i) \} \quad , \qquad (3.11)$$

$$\Theta = \frac{\pi}{2} \left\{ 1 + \sigma \frac{F(\xi, b_i)}{K(b_i)} \right\} + \frac{\pi}{2} (1-\sigma) \quad , \qquad (3.12)$$

$$\Omega(I) = \frac{\pi}{2K(b_i)} \quad , \qquad (3.13)$$

where the modulus b_i and the amplitude ξ are defined as

$$b_i^2 \equiv \frac{1+W}{2} \quad , \ (0 \leq b_i < 1) \quad , \qquad (3.14)$$

$$\sin \xi \equiv \frac{1}{b_i} \sin \frac{\chi}{2} \quad , \qquad (3.15)$$

and outside the separatrix,

$$I = \frac{8}{b_o \pi} E(b_o) \quad , \qquad (3.16)$$

$$\Theta = \frac{\pi}{2} \left\{ 1 + \sigma \frac{F(\xi, b_o)}{K(b_o)} \right\} + \frac{\pi}{2} (1-\sigma) \quad , \qquad (3.17)$$

$$\Omega(I) = \frac{\pi}{2 b_o K(b_o)} \quad , \qquad (3.18)$$

where the modulus b_o and the amplitude ξ are defined as

$$b_o^2 \equiv \frac{2}{1+W} \quad , \ (0 \leq b_o < 1) \quad , \qquad (3.19)$$

$$\xi \equiv \frac{X}{2} \quad . \qquad (3.20)$$

Here quantities K and E are complete elliptic integrals of the first and the second kind, respectively, and F is the incomplete elliptic integral of the first kind. The symbol σ represents 1 or -1 corresponding to the sign of velocity V:

$$\sigma \equiv \begin{cases} 1 \ , \ \text{for } V \geq 0 \ , \\ -1 \ , \ \text{for } V < 0 \ . \end{cases} \qquad (3.21)$$

The physical meaning of I is the area(which is devided by 2π) bounded by a particle trajectory inside the separatrix, or twice the area bounded by the X-axis and a trajectory outside the separatrix. Note that the actual angular velocity for a trapped particle is $\Omega(I)$, whereas that for an untrapped particle is $2\Omega(I)$. The relation between the coordinates (I,Θ) and (V,X) is demonstrated in Fig.6, and the angular velocity $\Omega(I/I_0)$ is exhibited in Fig.7. Here I_0 denotes the separatrix.

Then we consider the influence of the perturbation H_1 on the motion of a particle. By means of eq.(3.3), we obtain the equations of motion,

$$\frac{dI}{dT} = -\frac{\partial H_1}{\partial \Theta} \ , \qquad (3.22)$$

$$\frac{d\Theta}{dT} = \Omega(I) + \frac{\partial H_1}{\partial I} \ . \qquad (3.23)$$

Following B.V.Chirikov, E.Keil, and A.M.Sessler,[9] the second term

on the r.h.s. of eq.(3.23) can be neglected in analyzing particle trajectories near the separatrix. Then eq.(3.23) is integrated to give

$$\Theta = \Omega(I) T + \Theta_0 \quad . \qquad (3.24)$$

With the aid of eqs.(3.1) and (3.2), eq.(3.22) is expressed as

$$\frac{dI}{dT} = \frac{dI}{dH_0} \{ \frac{\partial H_0}{\partial X} \frac{dX}{dT} + \frac{\partial H_0}{\partial V} \frac{dV}{dT} \} \quad , \qquad (3.25)$$

$$= - \frac{\varepsilon}{\Omega(I)} V \sin X \cos T \quad . \qquad (3.26)$$

By means of Jacobian elliptic functions, the terms V and sinX in eq.(3.26) are expressed as functions of b_i, b_o, and ξ. With the aid of the series expansions[10] of Jacobian elliptic functions in terms of the nome q,

$$q \equiv \exp \{ - \frac{K(\sqrt{1 - b^2})}{K(b)} \} \quad , \qquad (3.27)$$

where b corresponds to b_i and b_o in each side of the separatrix, eq.(3.26) is described by action-angle variables I and Θ through b and ξ:

$$\frac{dI}{dT} = \varepsilon \sum_{n=-\infty}^{\infty} \Gamma_n(I) \sin \{ 2n\Theta - T \} \quad , \qquad (3.28)$$

where the Fourier amplitude Γ_n is

$$\Gamma_n(I) = 16\Omega^2 \frac{(-1)^n n^2 q^n}{1-q^{2n}} \quad . \qquad (3.29)$$

Thus we have obtained the basic equation (3.28) describing the influence of the perturbation on the motion of a particle.

Substituting eq.(3.24) into eq.(3.28) and integrating this equation, we obtain

$$\int dI = \int \varepsilon \sum_{n=-\infty}^{\infty} \Gamma_n(I) \sin\{2n\Omega(I)T - T + 2n\theta_0\}\, dT \quad . \qquad (3.30)$$

The non-zero contribution to this integral comes from the secular term where the condition $2n\Omega(I)-1 = 0$ holds, provided that the time variation of Γ_n through the variable I is negligibly small. Therefore we will define the k-th resonance surface I_k by the solution of the resonance condition:

$$2k\Omega(I) - 1 = 0 \quad . \qquad (3.31)$$

In the vicinity of I_k, the single resonance approximation is adopted, i.e., only the k-th harmonics on the r.h.s. of eq.(3.28) is retained and other terms are averaged out to zero, because the main contribution may be brought from the k-th harmonics. Following Y.Tomita, S.Seki, and H.Momota,[11] the first integral of the perturbed motion is described approximately by

$$\frac{1}{2}\frac{d\Omega}{dI}\Big|_{I=I_k}(I-I_k)^2 + \frac{\varepsilon}{2k}\Gamma_k(I_k)\cos\{2k\theta - T\} = \text{constant}, \qquad (3.32)$$

where the quantity Ω is linearized in the neighborhood of I_k. Then formation of an island in the vicinity of I_k is derived from the single resonance approximation.

The maximum extent $(\Delta I)_k$ of the k-th island is

$$(\Delta I)_k = 32k\left\{\varepsilon b_i^2(1-b_i^2)\frac{q^k}{1-q^{2k}}\frac{1}{I_k}\right\}^{\frac{1}{2}}, \qquad (3.33)$$

inside the separatrix, and

$$(\Delta I)_k = 32k\left\{\varepsilon\frac{1-b_o^2}{b_o^4}\frac{q^k}{1-q^{2k}}\frac{1}{I_k}\right\}^{\frac{1}{2}}, \qquad (3.34)$$

outside the separatrix. And correspondingly the frequency spread $(\Delta\Omega)_k$ of the k-th island is

$$(\Delta\Omega)_k = \frac{1}{4k^2}\left\{\varepsilon\frac{1}{b_i^2(1-b_i^2)}\frac{q^k}{1-q^{2k}}I_k\right\}^{\frac{1}{2}}, \qquad (3.35)$$

and

$$(\Delta\Omega)_k = \frac{1}{4k^2}\left\{\varepsilon\frac{b_o^4}{1-b_o^2}\frac{q^k}{1-q^{2k}}I_k\right\}^{\frac{1}{2}}. \qquad (3.36)$$

Chirikov's criterion is based on the idea of the overlapping of the neighboring islands. The evaluation function P called "the stochastic parameter" is defined as follows:

$$P(\varepsilon,k) \equiv \left| \frac{2(\Delta\Omega)_k}{(\delta\Omega)_{k,k+1}} \right| , \qquad (3.37)$$

where the quantity $(\delta\Omega)_{k,k+1} = |(\Delta\Omega)_k - (\Delta\Omega)_{k+1}|$ denotes the frequency spacing between two adjacent resonances. The stochastic parameter P may be applicable to the region where the resonance surfaces exist densely in order to determine the stochastic boundary. Then the quantity k may be regarded as continuous. And the application of the stochastic parameter may be restricted to the case where the inequality k>1 holds[9] because of the idea of the overlapping of adjacent islands. In each side of the separatrix, the value of ε which gives P=1 on the 1st resonance surface I_1 is approximately 0.014. For the value of ε larger than 0.014, the area bounded by the 1st resonance surfaces can be considered as the stochastic region. However, it may be misapplied in this case to use Chirikov's criterion for the purpose of obtaining the stochastic boundary.

Figure 8 demonstrates the discrepancy between the area of the stochastic region evaluated by Chirikov's criterion and the area estimated in Sec.2. Here the solid lines exhibit the boundaries obtained by Chirikov's criterion, the dotted lines exhibit the 1st resonance surfaces, and circles and squares correspond to the area estimated from Figs.3 (a) and (b), respectively.

4. Test particle Simulations

In this section, the appearance of the stochastic region and the dependence of this extent on the value ε are examined by means of the test particle simulations, i.e., the numerical integrations of eqs.(3.1) and (3.2) for various initial values and for various values of ε.

In order to visualize the stochastic and adiabatic regions, it is useful to introduce the surface of section plot. The surface of section plot is defined as a set of image points of Poincaré mappings. The results are demonstrated in Figs.9 (a)∿(f) in the action-angle coordinates. In these figures image points are plotted at the time $T=2n\pi$ $(n=0,1,2,.....,N)$ and the number N is chosen as 500.

In Figs.9 (a)∿(f), one may recognize the followings.

(a): ($\varepsilon=0.001$) The region bounded between the 2nd resonance surfaces($I_2=0.99981I_0$ and $1.00019I_0$ in each side of the separatrix) is stochastic, and the adiabatic islands appear in the vicinity of the 1st resonance surfaces. The stochastic region and the 1st adiabatic island are separated completely by an adiabatic layer in each side of the separatrix.

(b): ($\varepsilon=0.003$) The stochastic region and the region of the 1st adiabatic island increase gradually with the value of ε, and the adiabatic layer reduces its thickness.

(c): ($\varepsilon=0.006$) Outside the separatrix, the circumferential stochastic region of the 1st adiabatic island appears clearly.

But this stochastic region is isolated from the stochastic region in the vicinity of the separatrix. On the other hand, inside the separatrix the 1st adiabatic island is surrounded by the stochastic region including the separatrix. This is so-called resonance overlapping, i.e., the circumferential stochastic region of the 1st adiabatic island and the stochastic region near the separatrix are blended into one. The value of ε for this overlapping is different from that calculated in Sec.3. The extent of the 1st adiabatic island becomes smaller than that obtained from the single resonance approximation. The circumferential stochastic region may be a resultant stochastic region due to higher order resonances.

(d): (ε=0.009) As the value ε increases, the stochastic region becomes larger and the 1st adiabatic islands become much smaller.

(e): (ε=0.07) The 1st adiabatic islands vanish.

(f): (ε=0.3) At this large value of ε, another type of islands can be seen in the periphery of the stochastic region. It is clear that these islands result from higher order resonances.

Evolution of the stochastic region and the adiabatic islands obtained from the test particle simulations is illustrated in Fig.10. The values indicated in this figure are measured at $\Theta = 0$ inside the separatrix and $\Theta = \pi/2$ outside the separatrix. The region surrounded by a dotted curve in each side of the separatrix represents the extent of the 1st adiabatic island, and the hatched region is the stochastic region. The remaining region corresponds to the adiabatic region.

In order to compare these experimental results with theoretical ones, the extent of the 1st and 2nd islands are calculated. It is clear from the above-mentioned facts that the linearly evaluated extent of the islands, i.e., the expressions (3.33) or (3.34), does not coincide with the experimental results. Therefore the nonlinearly evaluated extent of the k-th island $(\Delta I_{N.L.})_k$ should be calculated. Practically the following expression may be useful:

$$\int \frac{\Omega(I) - \Omega(I_k)}{\Gamma_k(I)}\, dI + \frac{\varepsilon}{2k}\cos\{2k\theta - T\} = \text{constant}. \qquad (4.1)$$

In Fig.11 the nonlinearly evaluated extent of islands are shown, where the solid lines correspond to the 1st islands and the dotted lines to the 2nd islands. By comparing Fig.10 to Fig.11, the nonlinearly evaluated extent of the 1st and 2nd islands obtained from the single resonance approximation agrees quantitatively with experimental results. The squares in Fig.11 are the width of the stochastic region measured in the same manner employed in Fig.10. In the range $0.001 \lesssim \varepsilon \lesssim 0.005$, the width of the stochastic region is larger than the value I_2 by the amount $(\Delta I_{N.L.})_2$ in each side of the separatrix, and the 1st adiabatic islands are isolated. At $\varepsilon \sim 0.005$, the overlapping of the 1st and 2nd islands takes place. Then particles in the circumferential stochastic region of the 1st island, which is isolated

from the stochastic region near the separatrix at smaller values of ε, become to wander about the stochastic region near the separatrix. As the value ε increses from 0.005, the width of the stochastic region begins to enlarge abruptly because of the growth of the lst island itself and the growth of the circumferential stochastic region of the lst island. Consequently for the large value of ε, the width of the stochastic region is evaluated by $|I_0-I_1-(\Delta I_{N.L.})_1|$ inside and outside the separatrix.

5. Results and Discussions

In Sec.2 the self-consistent particle simulations have been executed and the phase trajectories of particles were examined. In the vicinity of the separatrix, it was observed that a group of particles exhibits stochastic motions and the particle distribution tends to be flat. Then the area of the stochastic region was estimated.

An application of Chirikov's criterion for estimating the stochastic boundary is limited only to the case of small ε. This was discussed in Sec.3. A discrepancy between the area of the stochastic region evaluated by Chirikov's criterion and that observed in Sec.2 has been exhibited.

In Sec.4, the process of growing the stochastic region has been visualized and the dependence of the width of the stochastic region on the value ε was obtained by means of the test particle simulations. These results coincided with theoretical ones

quantitatively, and supported the idea of the overlapping of adjacent islands. In the range $0.001 \lesssim \varepsilon \lesssim 0.005$, the 1st islands were the isolated ones and the width of the stochastic region was evaluated by I_2 and $(\Delta I_{N.L.})_2$. At $\varepsilon \sim 0.005$, the overlapping of this stochastic region and the circumferential stochastic region of the 1st island took place, and above this value of ε the width of the stochastic region was evaluated by I_1 and $(\Delta I_{N.L.})_1$. The discrepancy of the area of the stochastic region exhibited in Fig.8 was explained by this extent of the first island $(\Delta I_{N.L.})_1$.

Conseqently the following are inferred in the range $\varepsilon \ll 1$. When the stochastic region contains k-th and upwards ($k \gg 1$) resonance surfaces, and the (k-1)-th resonance surface is isolated, the width of the stochastic region is evaluated by I_k and $(\Delta I_{N.L.})_k$. If ε becomes a little larger, the overlapping of the stochastic region and the (k-1)-th island takes place, then, after some transition interval of ε, the width of the stochastic region becomes to be evaluated by I_{k-1} and $(\Delta I_{N.L.})_{k-1}$. At the same time $(\Delta I_{N.L.})_k$ is approximately $(\Delta I)_k$ due to the fact that for small ε the extent of an island is sufficiently small, so Chirikov's criterion P=1 evaluate accurately the area of the stochastic region.

In Sec.3, only the k-th harmonics were caluculated and the residual harmonics were averaged out to zero. However these residual harmonics act on the k-th island (which is generally called "primary island") as perturbations. By the application of the same analysis in Sec.3, it may be obvious that these perturbations introduce "secondary islands" and the stochastic

region in the vicinity of the separatrix of the k-th island. These types of the stochastic regions and islands were cleary observed in Fig.9 (c) (the circumferential stochastic region in the vicinity of the primary island) and in Fig.9 (f) (secondary islands). Because of exsistence of these higher order resonances, the width of the stochastic region exceeds that obtained from eq.(4.1) at the large value of ε.

Acknowledgements

The authors would like to express their sincere thanks to Dr. H. Naitou and Dr. H. Abe for their valuable discussions and technical suggestions. They also thank to Prof. Y. Midzuno for his encouragements.

References

1) T.M.O'Neil : Phys. Fluids 8, 2255 (1965).

2) M.N.Bussac, I.Mendonca, R.Pellet and A.Roux : Phys. Rev. Lett. 5, 349 (1974).

3) G.M.Zaslavskii and N.N.Filonenko : Sov. Phys. JETP 27, 851 (1968).

4) G.P.Berman and G.M.Zaslavskii : Sov. J. Plasma Phys. 3, 744 (1977).

5) G.R.Smith and N.R.Pereira : Phys. Fluids 21, 2253 (1978).

6) A.B.Rechester and T.H.Stix : Phys. Rev. A 19, 1656 (1979).

7) G.M.Zaslavskii and B.V.Chirikov : Sov. Phys. USPEKHI 14, 549 (1972).

8) B.V.Chirikov : Phys. Reports 52, 263 (1979).

9) B.V.Chirikov, E.Keil and A.M.Sessler : J. Statist. Phys. 3, 307 (1971).

10) M.Abramowitz and I.A.Stegun : Handbook of Mathematical Functions (Dover Pub. Inc., New York, 1970), p.575.

11) Y.Tomita, S.Seki and H.Momota : J. Phys. Soc. Japan 42, 687 (1977).

Figure Captions

Fig.1 Time evolution of the amplitude of an applied electrostatic wave. The initial amplitude Φ_0 is chosen as

(a) $e\Phi_0=0.22T_e$ (a small amplitude case), and

(b) $e\Phi_0=0.56T_e$ (a large amplitude case).

Fig.2 Examples of phase trajectories of electrons in a self-consistent field for

(a) a small amplitude case (Fig.1 (a)) and

(b) a large amplitude case (Fig.1 (b)).

The motions of type (i) are adiabatic, and type (ii) are stochastic. The dotted curves stand for the separatrix of the asymptotic amplitude Φ_∞.

The initial values of (x,v) are as follows:

(a): (i) $(16.0,-0.2V_t)$ and $(16.0,-1.0V_t)$

(ii) $(8.0,-0.66V_t)$

(b): (i) $(16.0,-0.4V_t)$ and $(16.0,-1.8V_t)$

(ii) $(8.0,-0.2V_t)$

Fig.3 The stochastic region in the self-consistent field (Fig.1) evaluated by the wave after initial one period for (a) a small amplitude case and (b) a large amplitude case. The dotted curves correspond to the separatrix of Φ_∞. The area is estimated approximately as follows:

(a) $0.34I_0$(inside the separatrix)

$0.19I_0$(outside the separatrix)

(b) $0.35I_0$ (inside the separatrix)

$0.27I_0$ (outside the separatrix)

Fig.4 The initial Maxwellian distribution observed in the unperturbed wave frame.

Fig.5 Time evolution of distributions of electrons in the phase plane for (a) a small amplitude case and (b) a large amplitude case.

T_1: after initial one period of the amplitude oscillation.

T_2: a half period after T_1.

Final: the final state.

Fig.6 The relation between the coordinates (I,Θ) and (V,X). The line $I=I_0$ is the separatrix.

Fig.7 The angular velocity $d\Theta/dT = \Omega(I/I_0)$.

Fig.8 The area of the stochastic region evaluated by Chirikov's criterion and that estimated from Figs.3 (a) and (b): The solid lines are the stochastic boundaries determined by Cirikov's criterion. The dotted lines stand for the 1st resonance surfaces. Circles correspond to the area estimated from Fig.3 (a) and squares to Fig.3 (b).

Fig.9 The surface of section plot in the action-angle coordinates. The values of ε are as follows.

(a) : 0.001 (b) : 0.003 (c) : 0.006

(d) : 0.009 (e) : 0.07 (f) : 0.3

Fig.10 Evolution of the stochastic region and the adiabatic islands: The values are measured at $\theta=0$ inside the separatrix and at $\theta=\pi/2$ outside the separatrix. The region surrounded by a dotted curve represents the extent of the 1st adiabatic island. The hatched region is the stochastic region.

Fig.11 The nonlinearly evaluated extent of the 1st (solid lines) and 2nd (dotted lines) islands: The squares show the width of the stochastic region measured in the same manner in Fig.10.

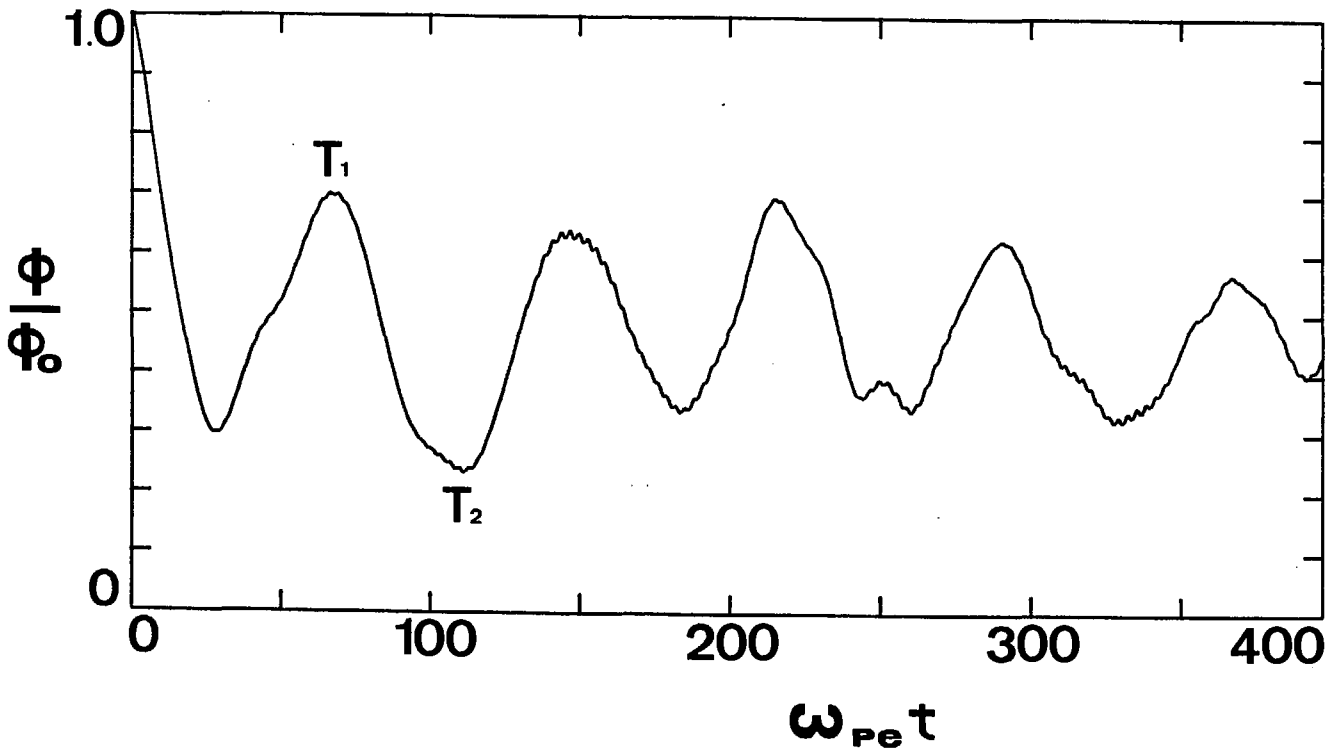

Fig. 1 (a)

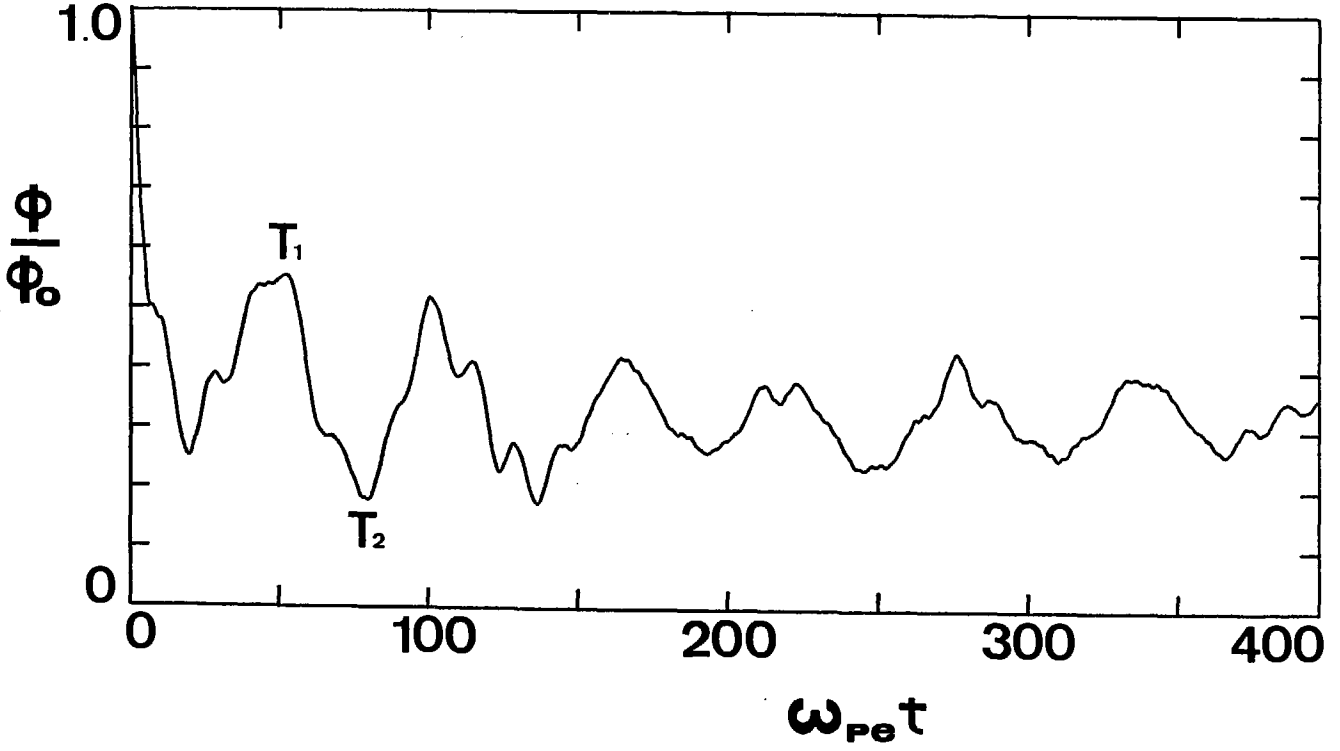

Fig. 1 (b)

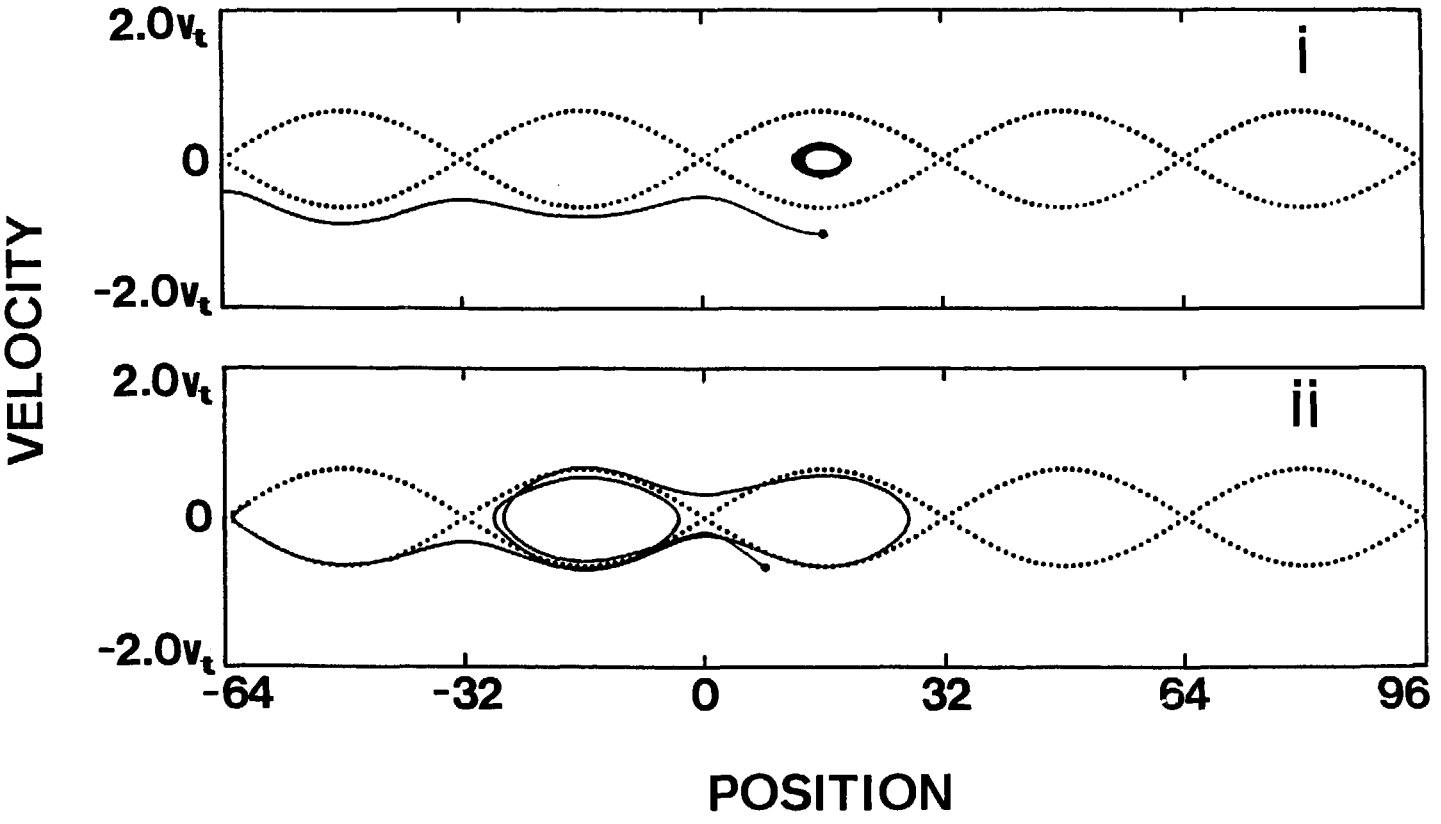

Fig. 2 (a)

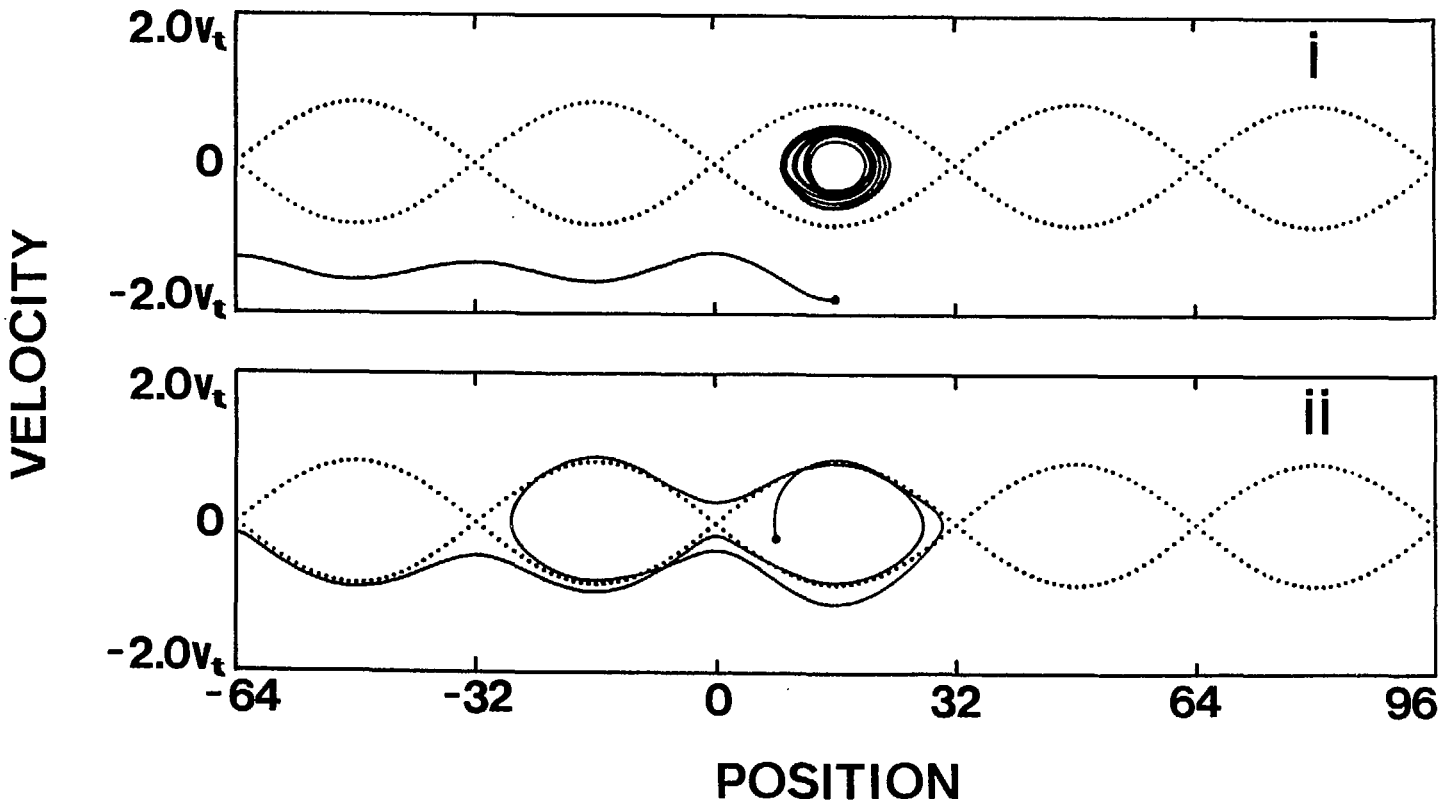

Fig. 2 (b)

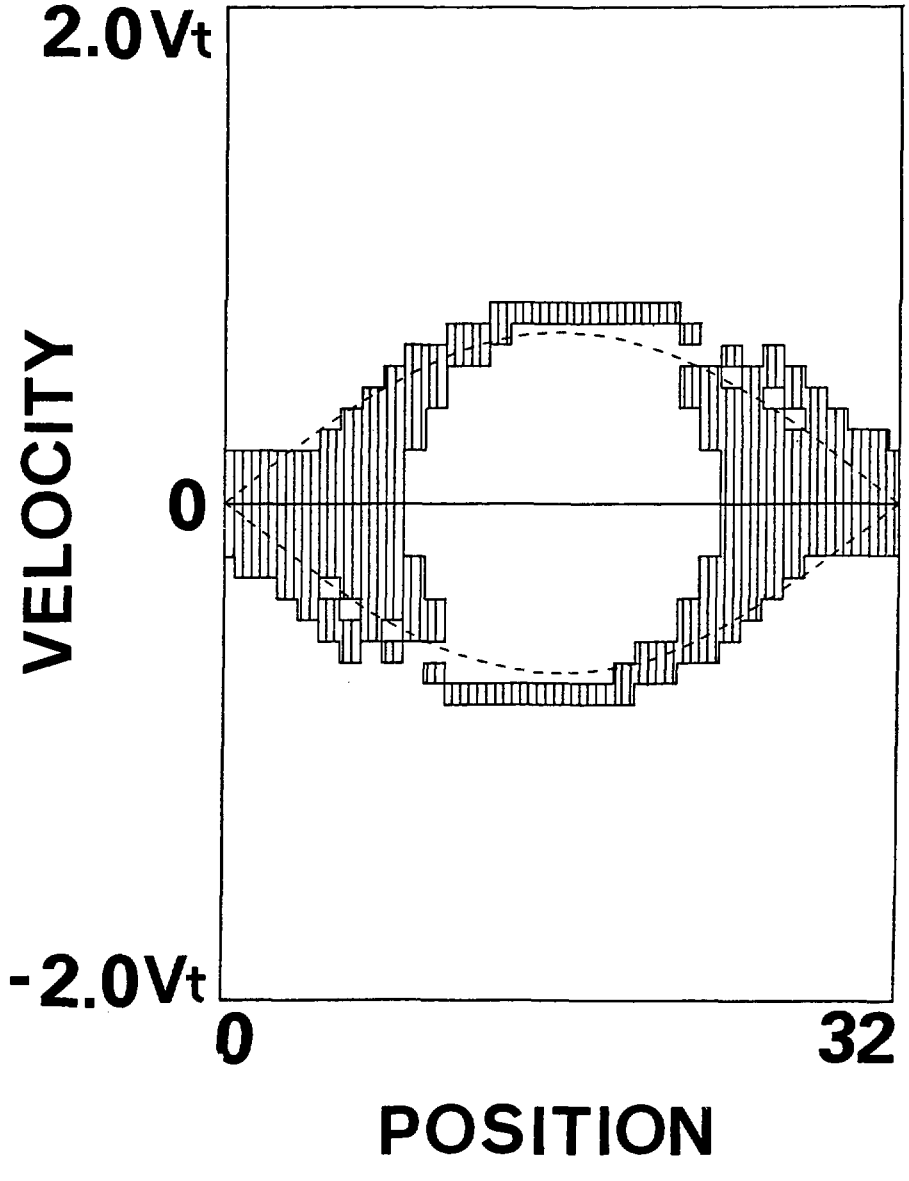

Fig. 3 (a)

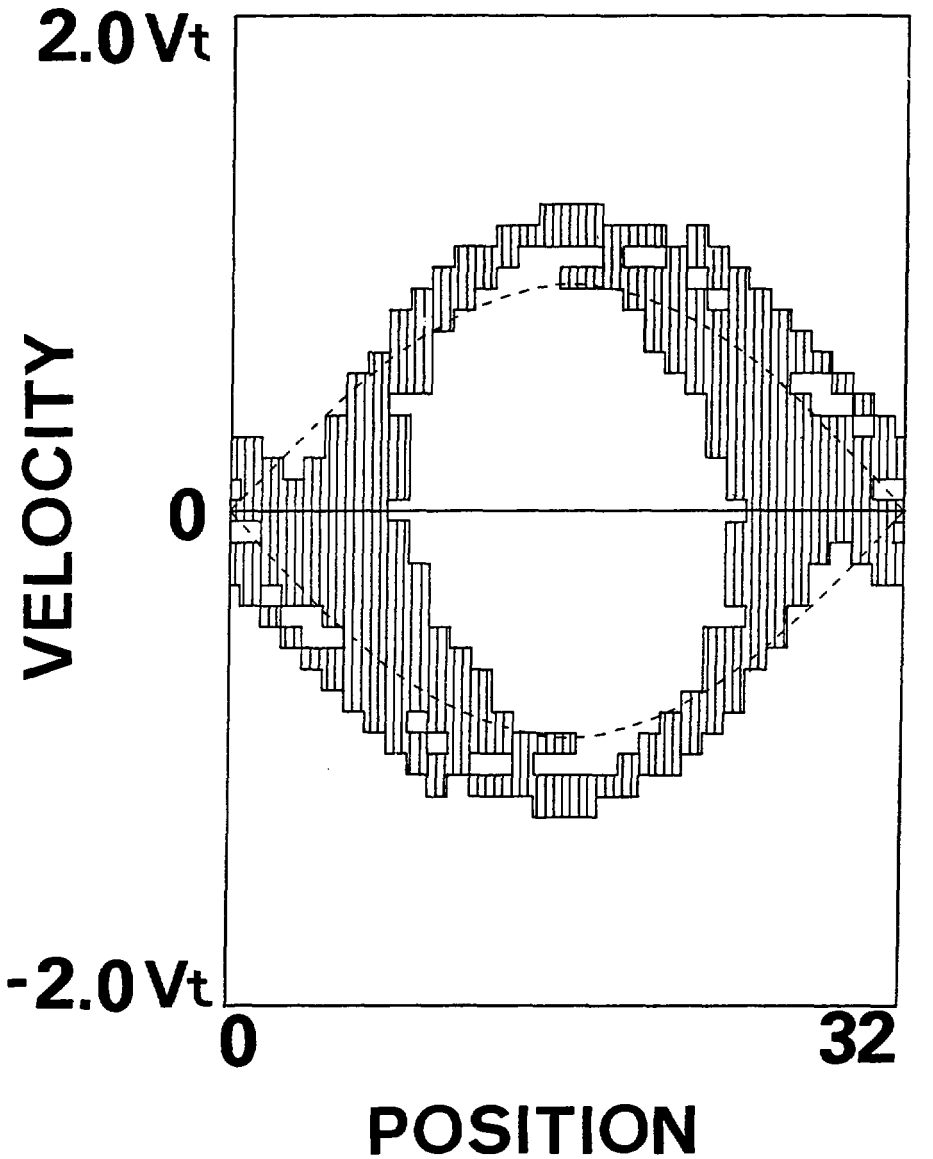

Fig. 3 (b)

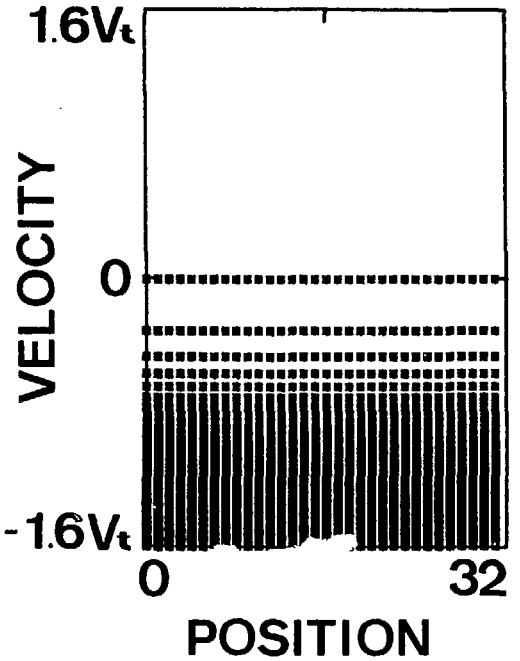

Fig. 4

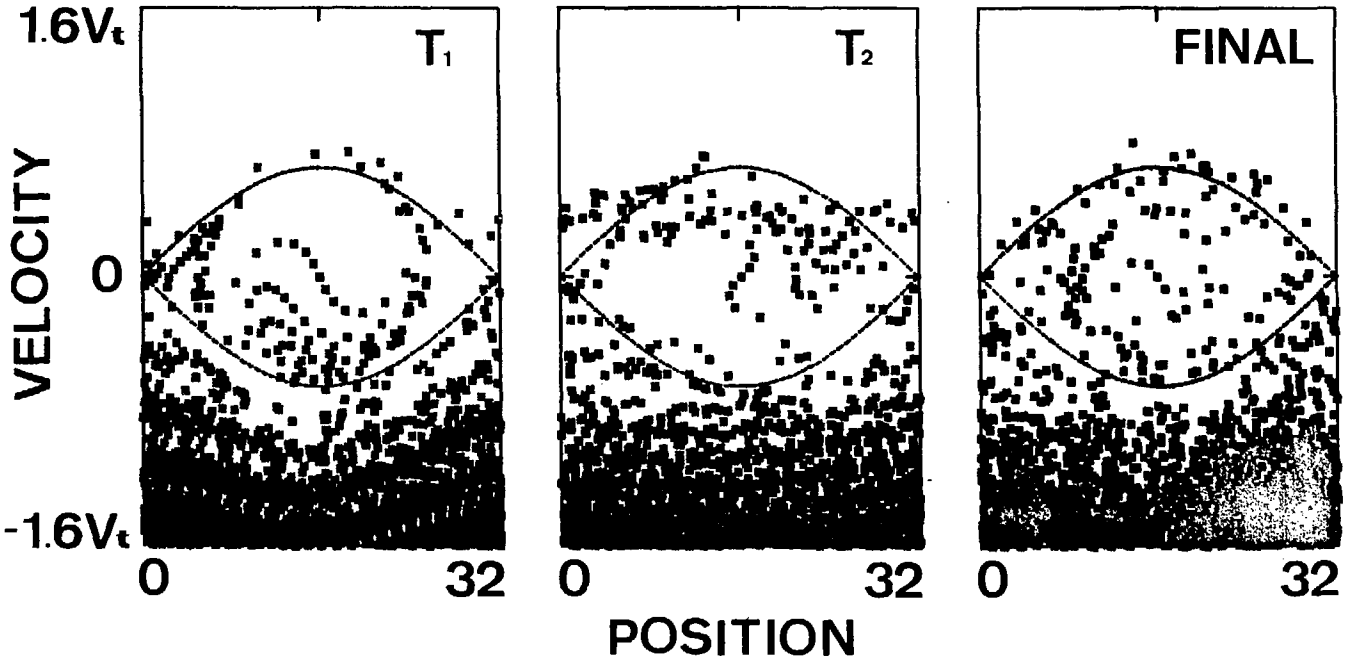

Fig. 5 (a)

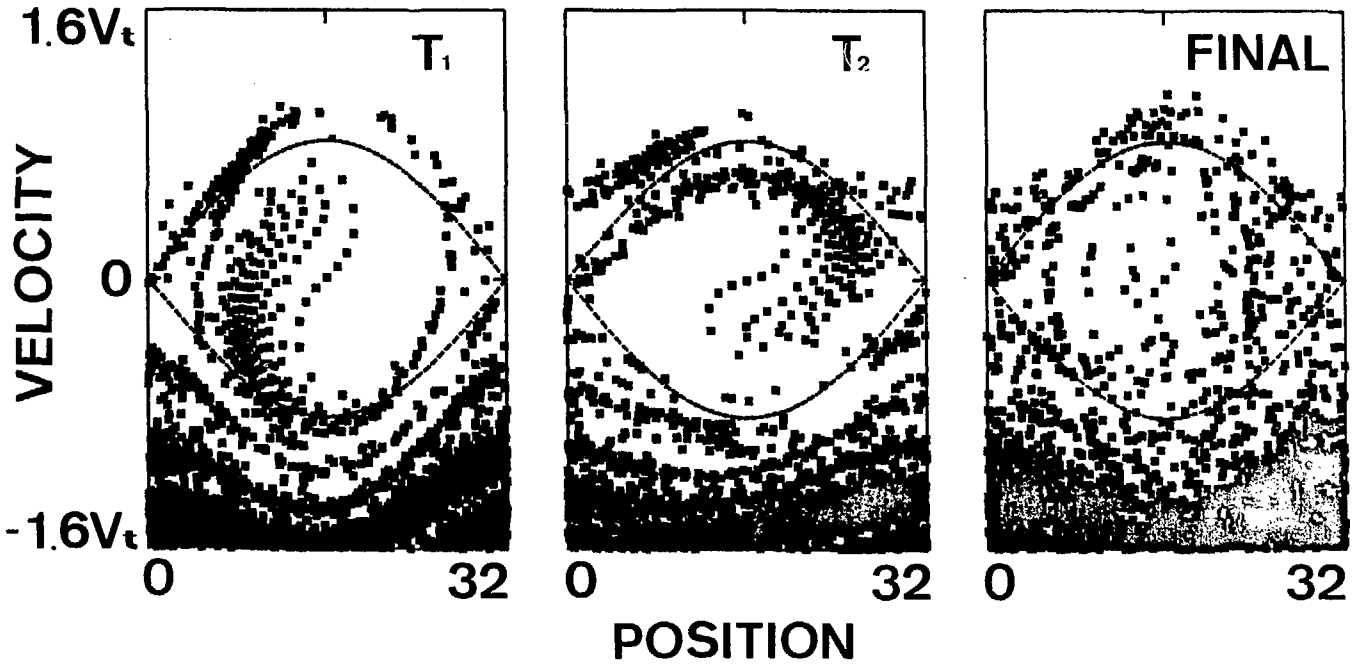

Fig. 5 (b)

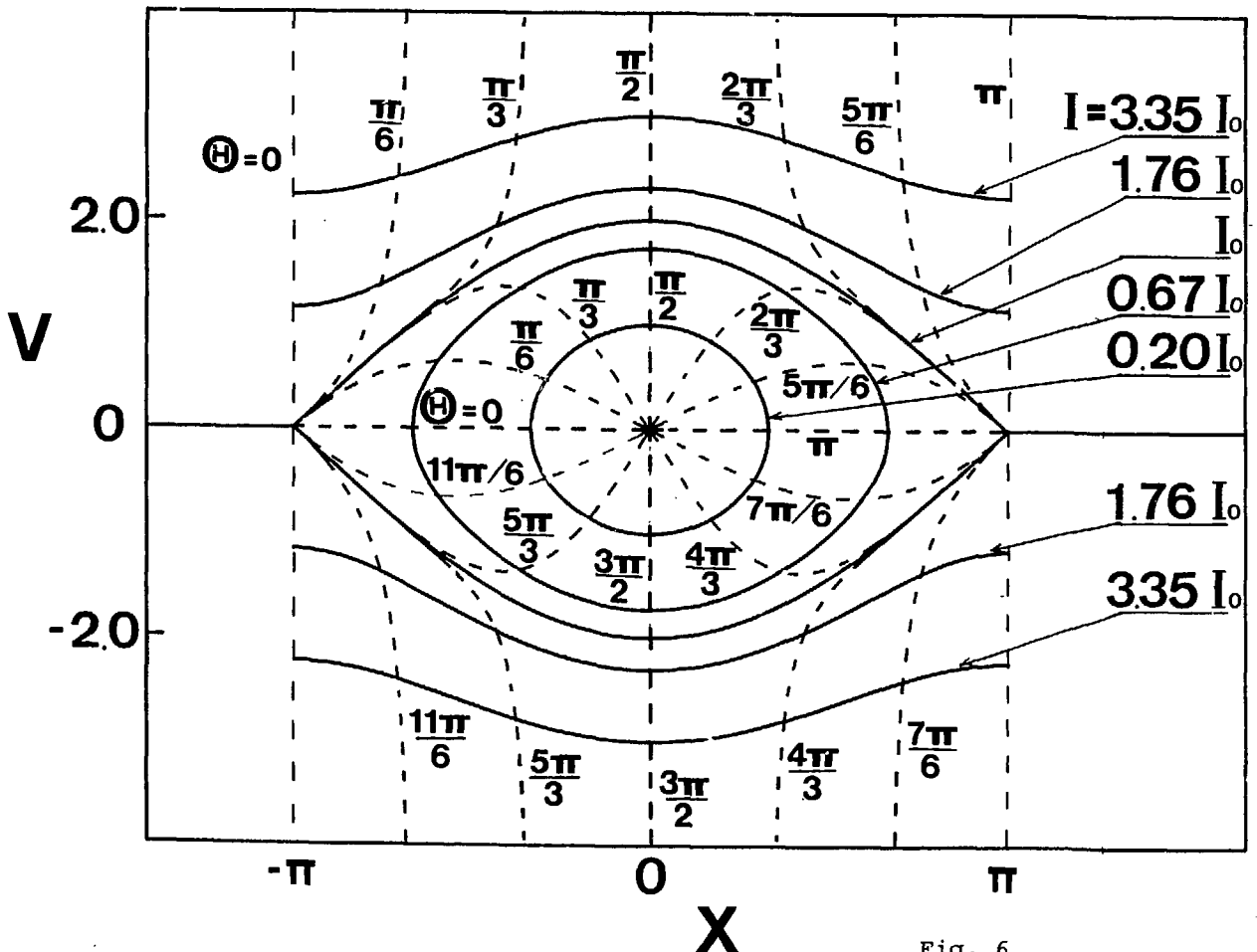
V
X
2.0
0
-2.0
-π
0
π
Θ=0
π/6
π/3
π/2
2π/3
5π/6
π
I=3.35 I₀
1.76 I₀
I₀
0.67 I₀
0.20 I₀
1.76 I₀
3.35 I₀
11π/6
5π/3
3π/2
4π/3
7π/6

Fig. 6

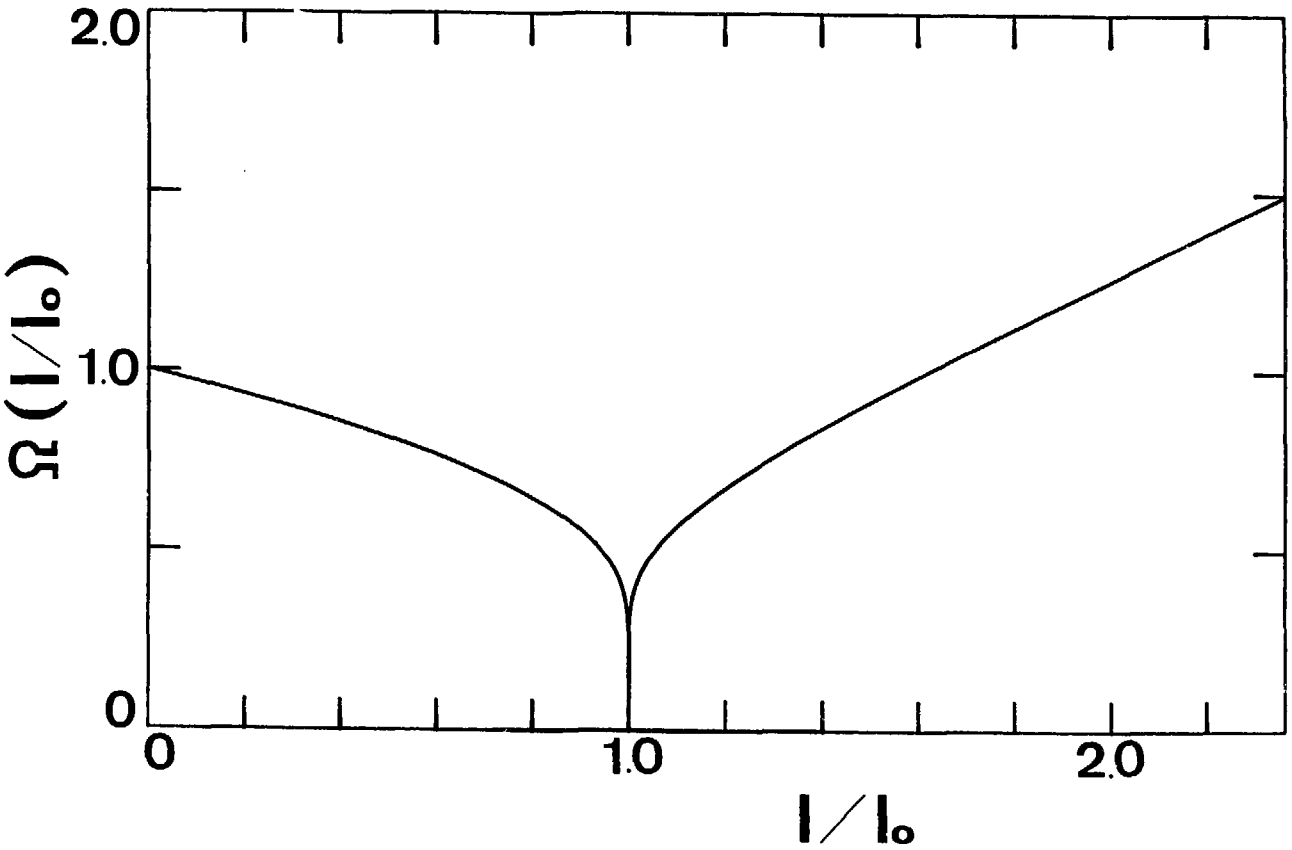

Fig. 7

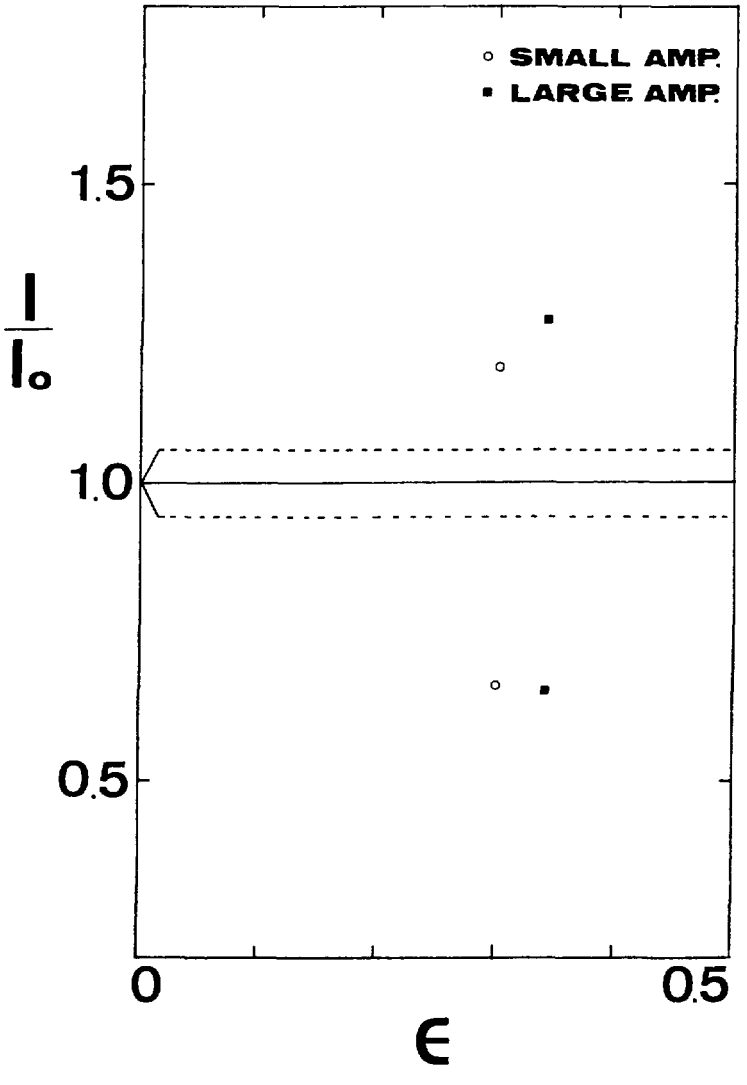

Fig. 8

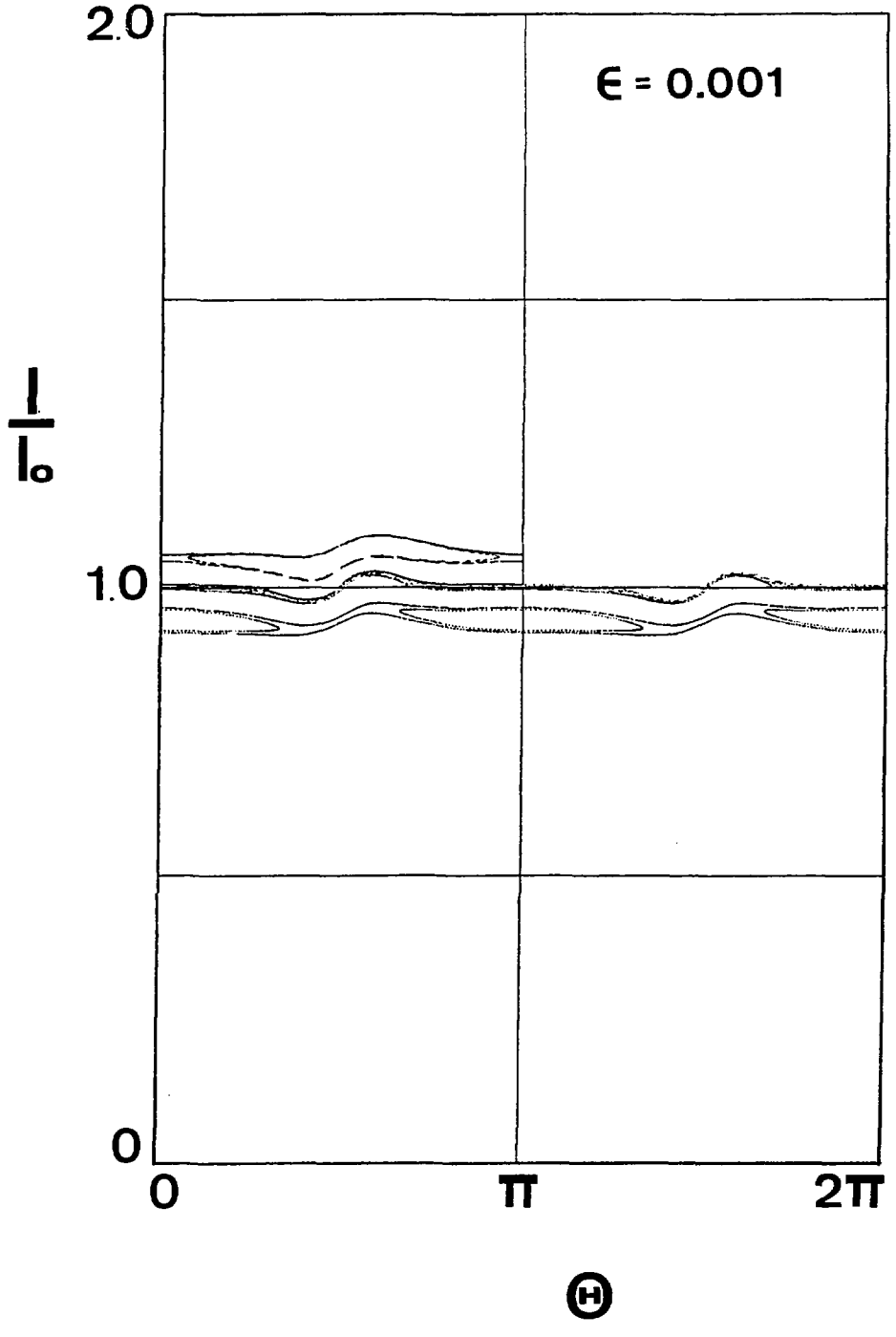

Fig. 9 (a)

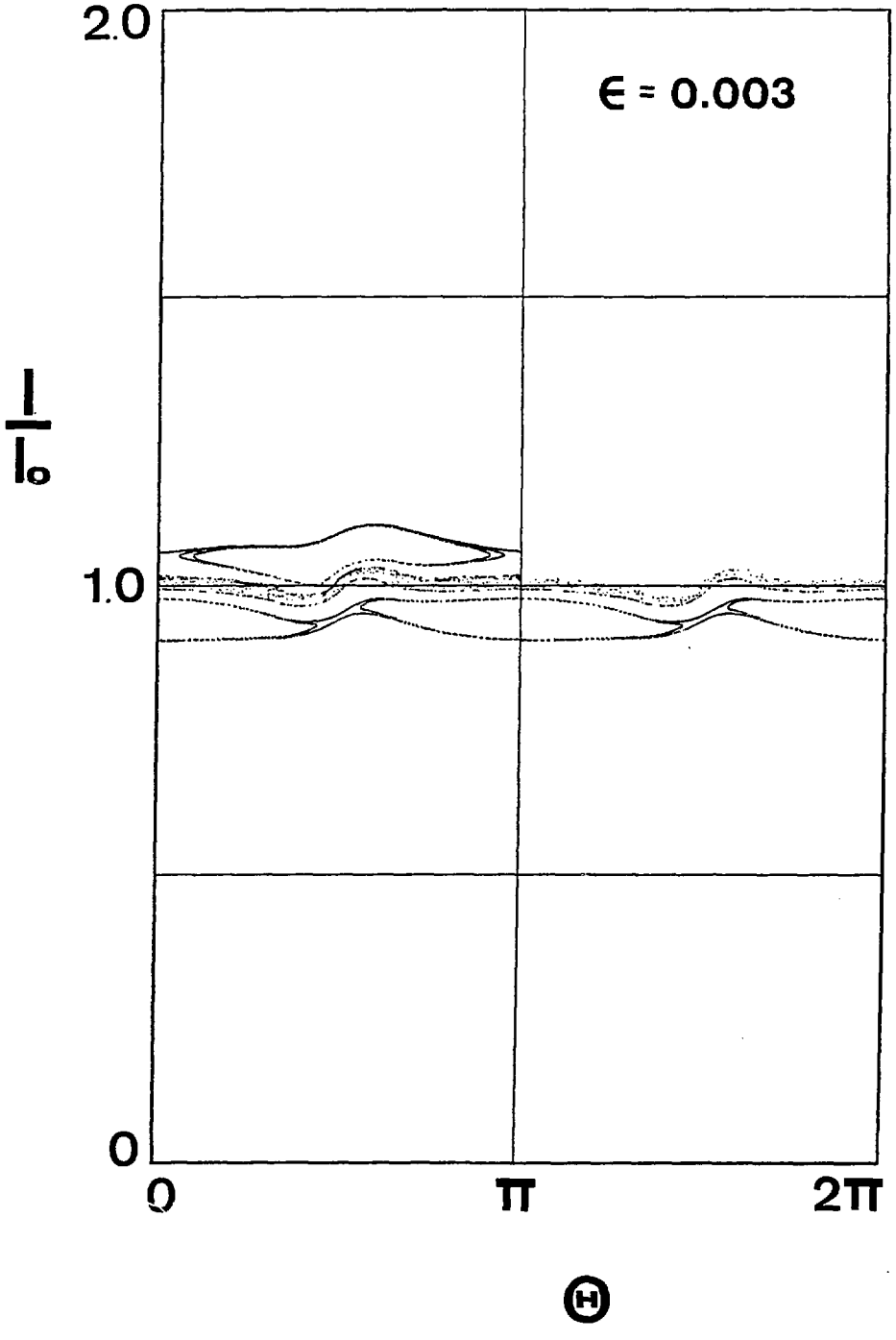

Fig. 9 (b)

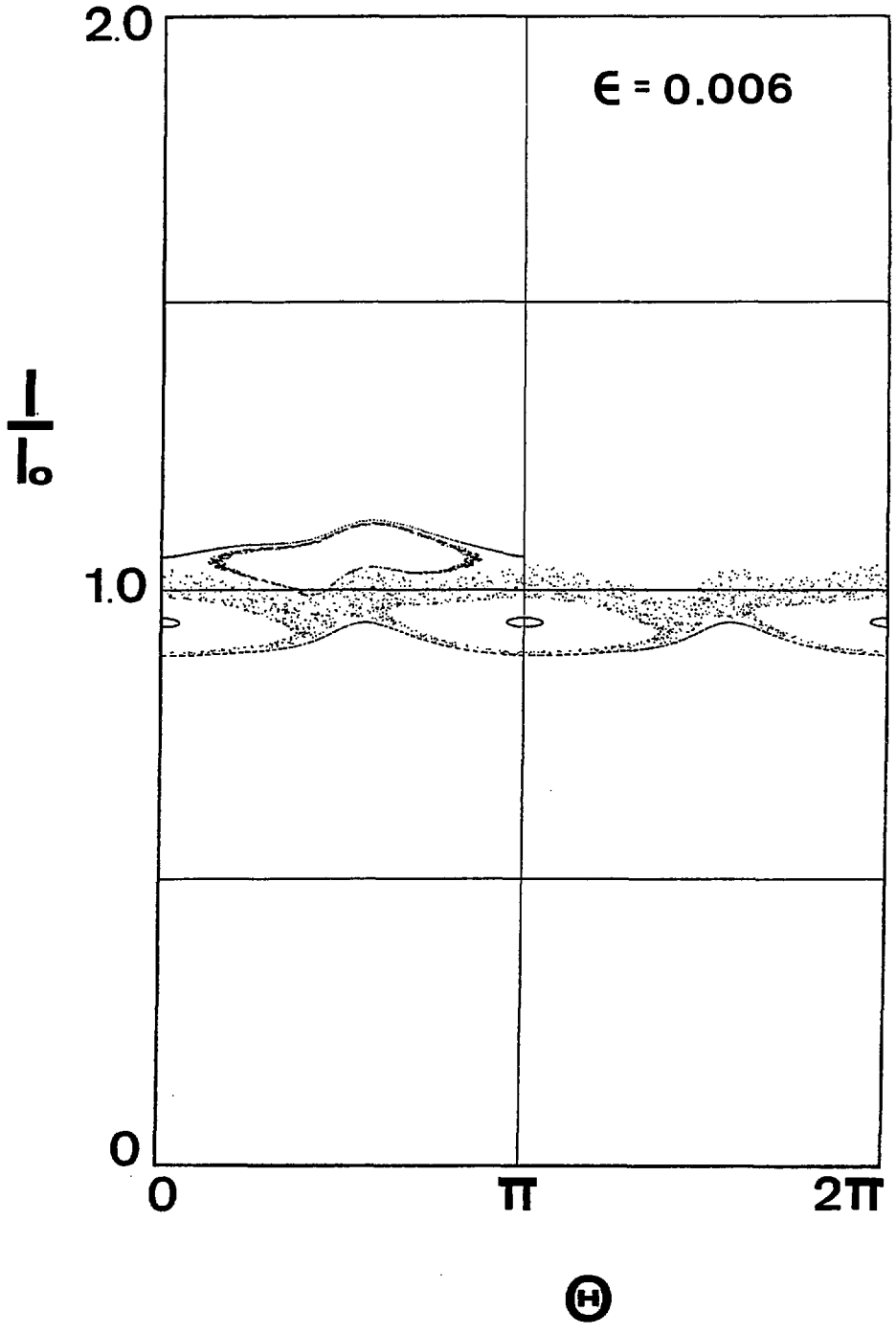

Fig. 9 (c)

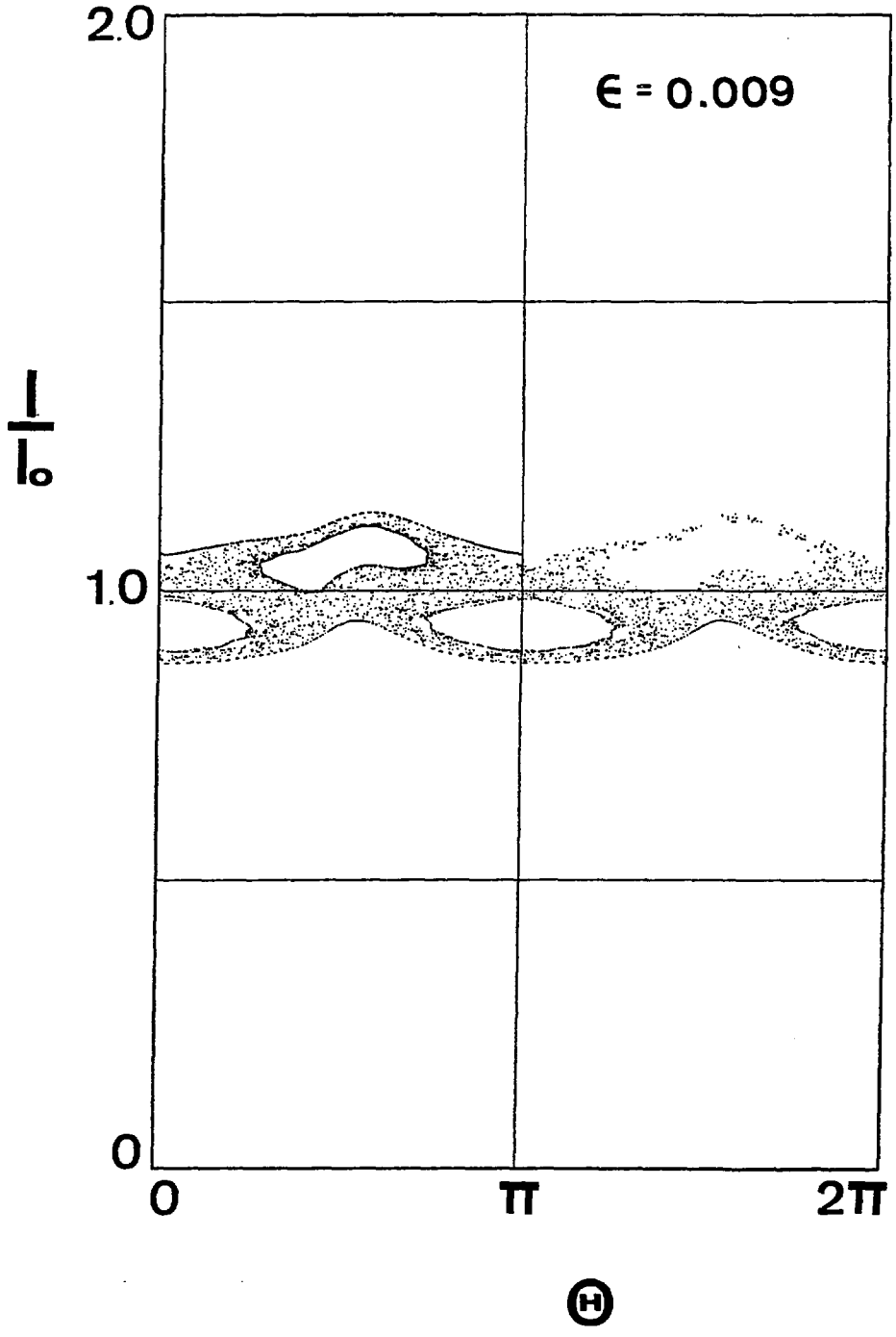

Fig. 9 (d)

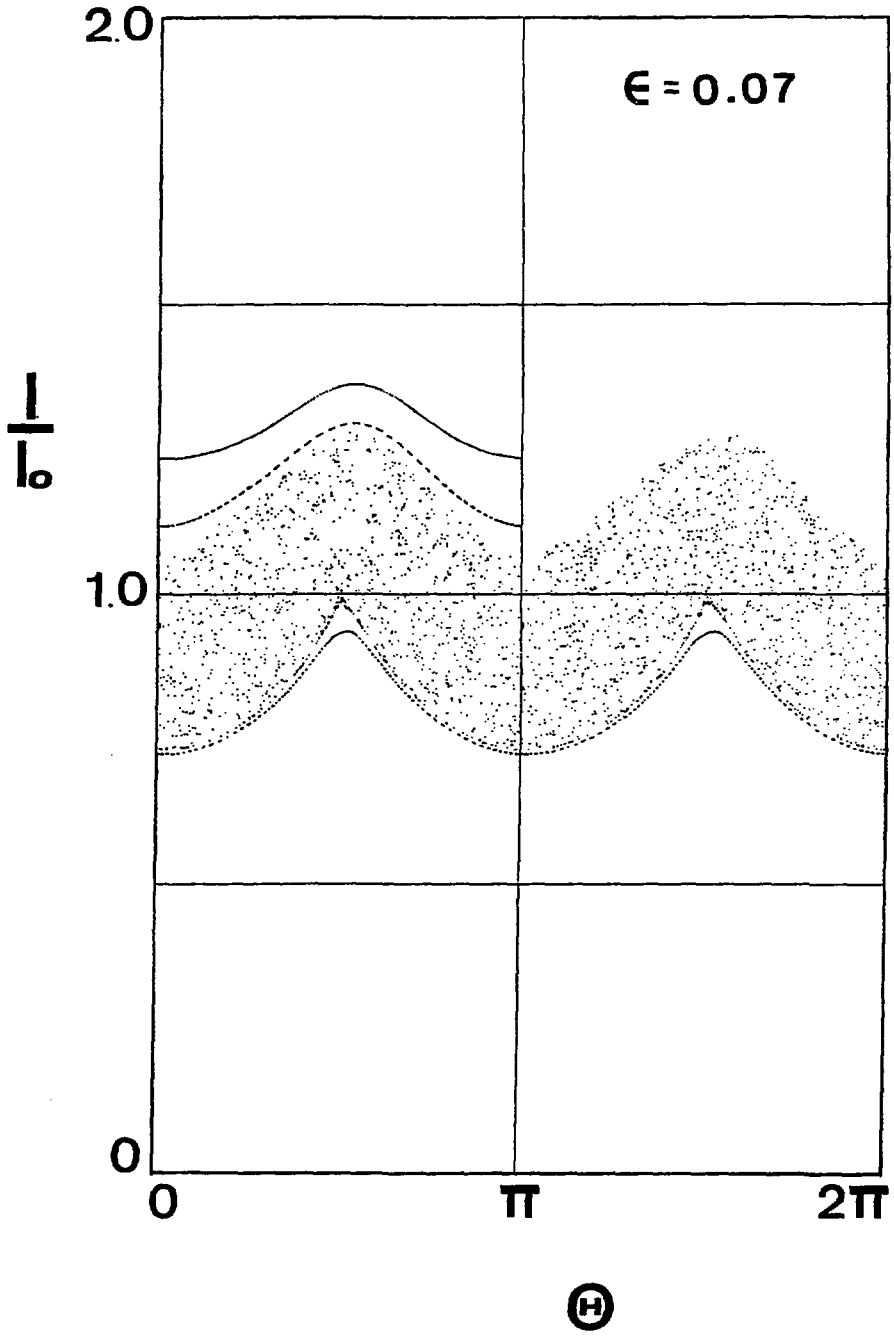

Fig. 9 (e)

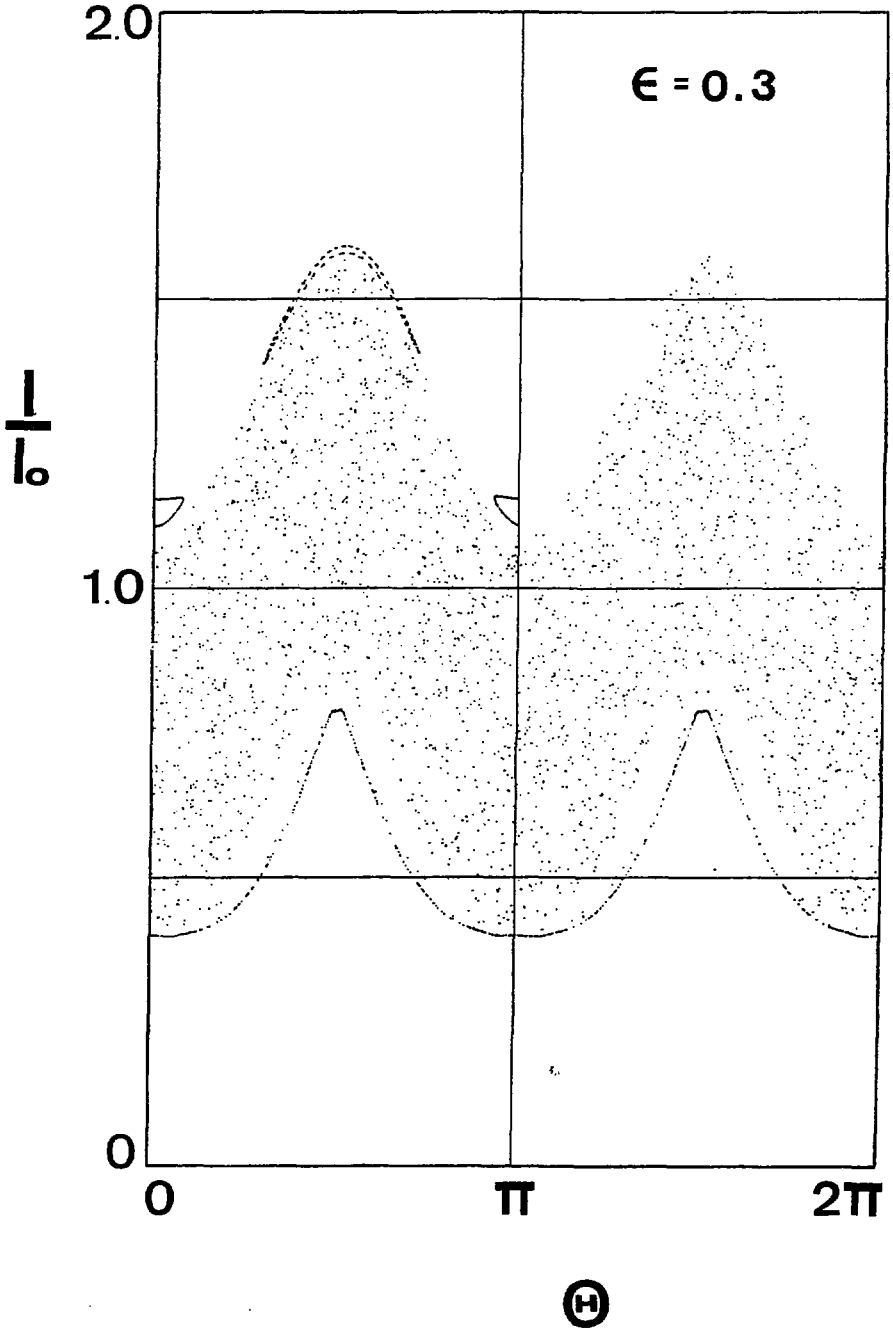

Fig. 9 (f)

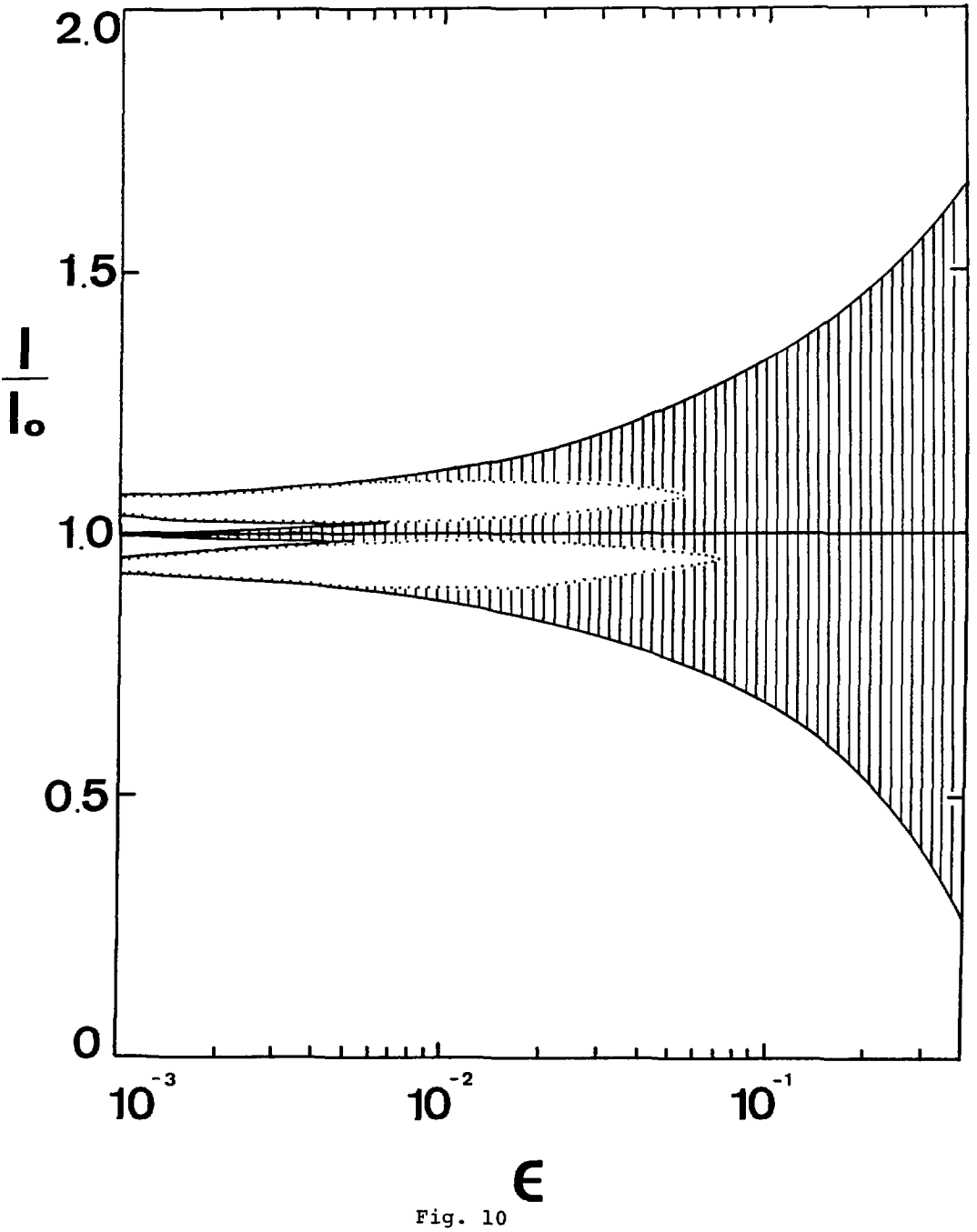

Fig. 10

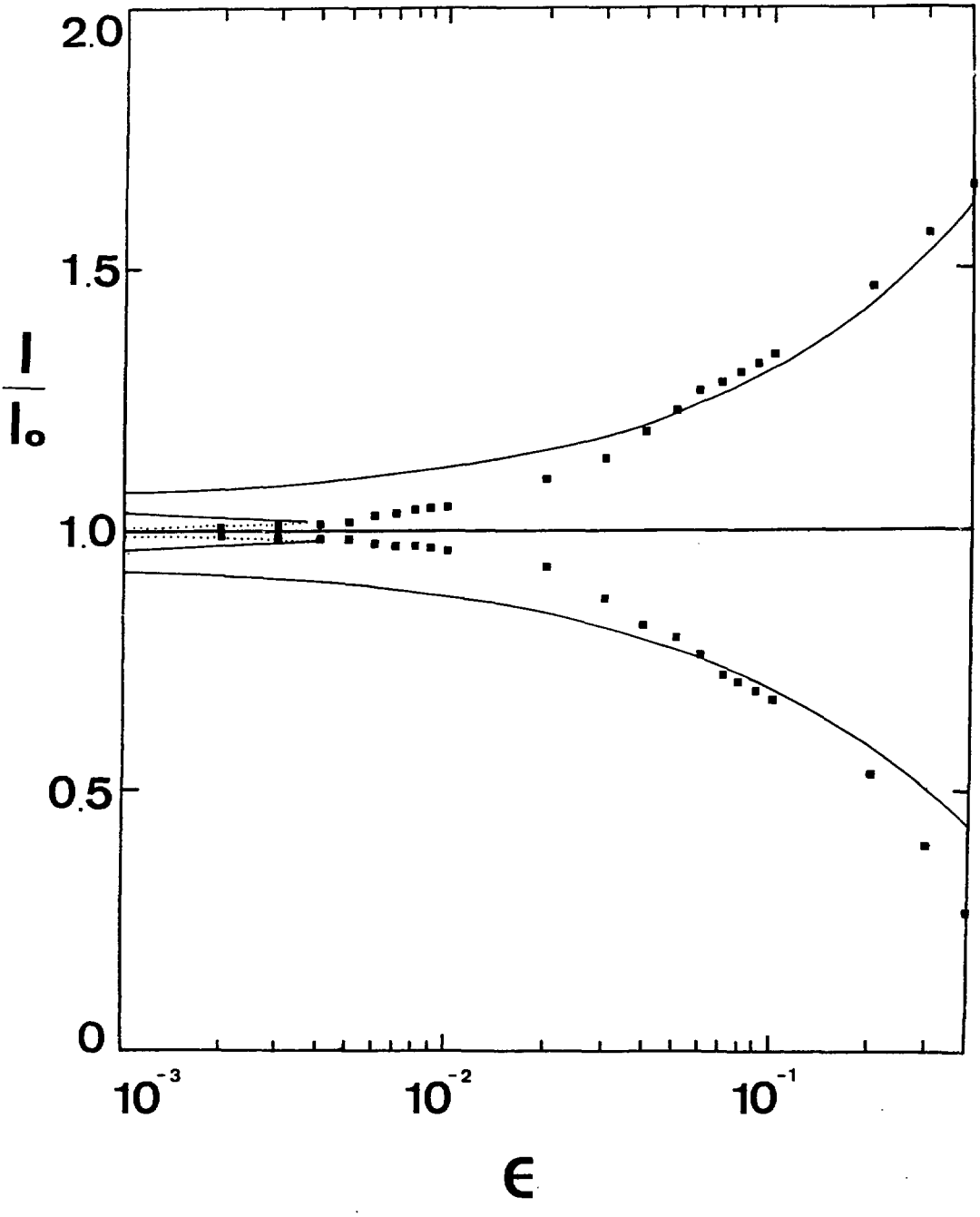

Fig. 11